Theoretical Study toward Understanding the Catalytic Mechanism of Pyruvate Decarboxylase

Jianyi Wang,[†] Hao Dong,[†] Shuhua Li,*[,†] and Hongwu He[‡]

Laboratory of Mesoscopic Chemistry, Institute of Theoretical and Computational Chemistry, Department of Chemistry, Nanjing University, Nanjing 210093, People's Republic of China, and Institute of Organic Synthesis Chemistry College, Central China Normal University, Wuhan, 430079, People's Republic of China

Received: May 26, 2005; In Final Form: August 3, 2005

Density functional calculations are employed to explore the mechanisms of all elementary reaction steps involved in the catalytic cycle of pyruvate decarboxylase (PDC). Different models are constructed for mimicking the involvement of some key residues in a certain step. The effect of the protein framework on the potential energy profiles of active site models is approximately modeled by fixing some freedoms, based on the crystal structure of the PDC enzyme from *Saccharomyces cerevisiae* (ScPDC). Our calculations confirm that Glu51 is the most important residue in the formation of the ylide and the release of acetaldehyde via the proton relay between Glu51, $N_{1'}$, and the 4′-amino group of thiamine diphosphate. The presence of Glu477 and Asp28 residues makes the decarboxylation of lactylthiamin diphosphate (LThDP) an endothermic process with a significant free energy barrier. The protonation of the α-carbanion to form 2-(1-hydroxyethyl)-thiamin diphosphate is found to go through a concerted double proton transfer transition state involving both Asp28 and His115 residues. The final step, acetaldehyde release, is likely to proceed through a concerted transition state involving carbon−carbon bond-breaking and the deprotonation of the α-hydroxyl group. The decarboxylation of LThDP and the protonation of the α-carbanion are two rate-limiting steps, relative to the facile occurrence of the ylide formation and acetaldehyde release. The catalytic roles of residues Glu51, Glu477, Asp28, and Gly417 in the active site of ScPDC in individual steps elucidated from the present study are in good agreement with those derived from site-directed mutagenesis.

1. Introduction

Pyruvate decarboxylase (PDC, E.C. 4.1.1.1) is the simplest thiamin diphosphate (ThDP)-dependent enzyme and is a key enzyme in alcohol fermentation.[1,2] This enzyme catalyzes the conversion of pyruvate to acetaldehyde and carbon dioxide. The X-ray structures of two PDC enzymes, from the yeast *Saccharomyces cerevisiae* (ScPDC) and the bacterium *Zymomonas mobilis* (ZmPDC), have been determined in the past decade. The active centers of two enzymes have similar three-dimensional structures, both of which require ThDP and Mg(II) ions as cofactors for catalytic activity. The ThDP binding site is highly similar in both ScPDC and ZmPDC. Most of the amino acids within the van der Waals distance (<3.8Å) to the thiazolium ring of ThDP are conserved in the yeast and *Z. mobiliz* enzymes (as shown in Figure 1), indicating that the catalytic cycles in both enzymes may be similar.[3] The commonly accepted mechanism[4] of the catalytic cycle of PDC (shown in Figure 2) includes (1) the abstraction of the proton from the C_2 atom of ThDP, (2) the binding of the substrate to yield the assumed intermediate, 2-lactylthiamin diphosphate (LThDP), (3) the decarboxylation of LThDP to form 2-(1-hydroxyethyl)-thiamin diphosphate (HEThDP), and (4) the release of acetaldehyde. Although extensive kinetic and mechanistic experiments have demonstrated that the isolated ThDP and related compounds can catalyze the decarboxylation of pyruvate at a very slow rate, the protein environment accelerates the overall enzyme reaction by a factor of 10^{12}−10^{13}.[5,6] Clearly, it is important to understand the role of the amino acids surrounding the coenzyme during catalysis.

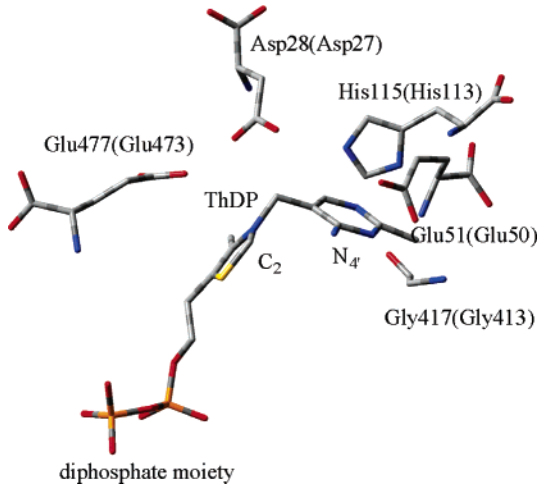

Figure 1. Crystal structure of the active site of ScPDC with the cofactor ThDP. For each conserved residue in ScPDC, its corresponding sequence number in ZmPDC is included in parentheses.

It has been recognized from the crystal structures of both ZmPDC and ScPDC that the diphosphate group and Mg^{2+} of the active site mainly play an anchoring function in the cofactor and are not directly involved in the catalytic reactions.[7] In the active center of the enzyme, the enzyme-bound ThDP is in a

* Author to whom correspondence should be addressed. E-mail: shuhua@nju.edu.cn.
[†] Nanjing University.
[‡] Central China Normal University.

10.1021/jp052802s CCC: $30.25
Published on Web 09/09/2005

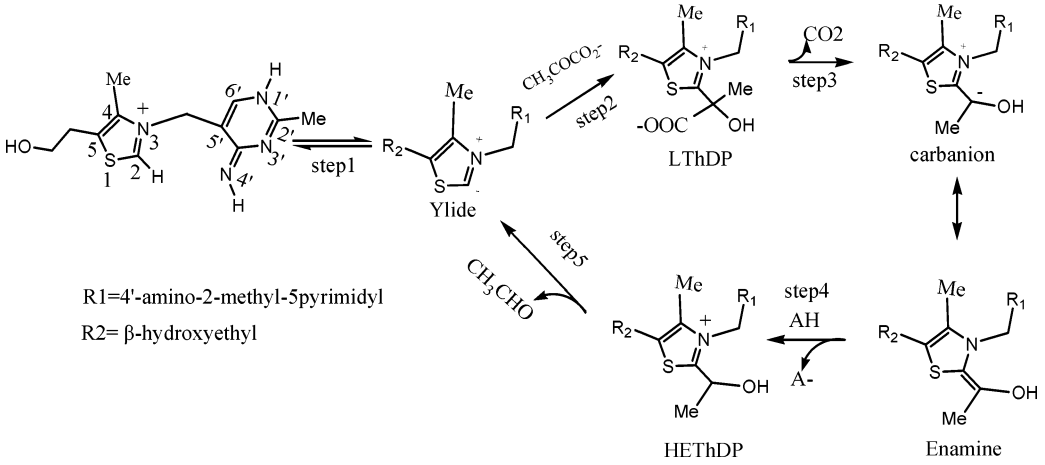

Figure 2. Proposed catalytic mechanism of PDC.

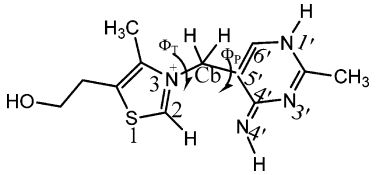

Figure 3. A schematic picture of the "V-like" thiamin. The conventional numbering of atoms in the two rings is given: $\Phi_P(C_{4'}-C_{5'}-C_b-N_3) = -65°$; $\Phi_T(C_{5'}-C_b-N_3-C_2) = 98°$.

typical "V" conformation,[8] with the torsion angles $\Phi_T \approx \pm 95°$ and $\Phi_p \approx \pm 70°$,[9] respectively (Figure 3). This conformation brings the $N_{4'}$ and C_2 atoms to within 3.5 Å of each other, a plausible distance for either direct or mediated proton transfer between the two atoms.[10,11] Recent studies revealed that the deprotonation step of the C_2 atom is catalyzed by the interaction between the glutamate (Glu51) residue and the $N_{1'}$ atom in the pyrimidine ring of ThDP, leading to the increased basicity of the 4′-amino group.[12,13] On the basis of the distribution of covalent intermediates measured by ^{1}H NMR spectroscopy in wild-type ZmPDC and its variants, Jordan et al. provided clear evidence that the four residues Asp27, Glu50, His113, and Glu473, close to the enzyme-bound ThDP, all have dramatic effects on the whole catalytic cycle.[14−17] Specifically, in the substrate-binding step, the proton relay between Glu50, $N_{1'}$, and the 4′-amino group of ThDP protonates the carbonyl oxygen of the substrate, and the presence of Glu 473 is important in the optimal orientation of the substrate. In the last step, the release of acetaldehyde requires the protonation of the α-carbanion and the deprotonation of the α-hydroxyl group of HEThDP. Both His113 and Asp27 groups were found to be involved in the protonation of the α-carbanion, whereas Glu50 has a drastic effect on the rate of acetaldehyde release probably through affecting the deprotonation of the α-hydroxyl group of HEThDP.[14] To conclude, recent experimental results[15−18] have enabled the assignment of individual side chains to each step in catalysis and provided important insight into the reaction mechanism of PDC at a molecular level.

However, several theoretical studies on some reaction steps of the catalytic cycle of PDC by using various models appeared. Early theoretical calculations were carried out to understand the electronic structures of thiamin-related compounds.[19] Friedemann and Breitkopf[20] have performed molecular mechanics and semiempirical AM1 and PM3 calculations on the adduct of ThDP with the substrate pyruvate and its decarboxylation products. The barrier for the decarboxylation process obtained by PM3 calculations was estimated to be about 4.0 kcal/mol without the presence of residues. Sakaki et al.[21] have studied the decarboxylation reaction of 2-lactylthiazolium (a simple model of LThDP) with AM1 and ab initio HF or MP2 methods. The calculated activation barrier is 1.5 kcal/mol by AM1 and 4.4 kcal/mol by MP2/6-31G, while the calculated exothermicity is 23.8 kcal/mol (AM1). However, the interaction of several water molecules with 2-lactylthiazolium increases the activation barrier to 19.0 kcal/mol (AM1) and even changes the exothermicity from 23.8 to −2.1 kcal/mol (i.e., the reaction becomes endothermic). This study revealed that the presence of active site residues might have significant impact on the energetics of the decarboxylation process of LThDP. Recently, Friedemann et al. studied the effect of $N_{1'}$ protonation on the structures and the electronic properties of thiamin and 2-hydroxyethyl-thiamin carbanion by using density functional theory (DFT) calculations.[14,22,23] Their calculations supported the experimental findings that the acidity of the 4′-amino group is significantly enhanced by the $N_{1'}$ protonation of thiamin species. Moreover, they found that the protonation of the $N_{1'}$ position could reduce to some extent the barrier of the proton transfer from the 4′-amino group to the carbanion center. In addition, molecular dynamics simulations have been carried out to model the effect of residues of the apoenzyme to the structure of the coenzyme.[24] However, we notice that a systematic theoretical study on the whole catalytic cycle of PDC has not been done before. Especially, the molecular mechanism of how some key residues contribute to a certain step has not been explored theoretically.

In this article, our aim is to theoretically investigate the mechanism of all elementary reaction steps involved in the catalytic cycle of PDC by high-level DFT calculations. The models considered in this work, which are constructed on the basis of the crystal structure of ScPDC, are more realistic than those used in previous theoretical studies.[20−26] For each reaction step, a minimum realistic model is constructed, which includes some key residues to the studied reaction. The rest apoenzyme environment is treated as a dielectric continuum and its effect on each catalytic step is calculated by the self-consistent reaction field method. An advantage of such a theoretical study is that the specific contribution of different residues to a certain reaction step can be understood.

2. Computational Details

All of the calculations have been performed with Gaussian 03 program package.[27] Density functional theory was employed with the three-parameter hybrid exchange functional of Becke and the Lee, Yang, and Parr correlation functional (B3LYP). The 6-31G(d,p) basis set was employed for all geometry

optimizations. Constrained geometry optimizations have been performed to obtain the structures of reactants, intermediates, transition states, and products. Since the V-like conformation of the enzyme-bound ThDP enforced by the protein framework is important for its catalytic activity, we have frozen two characteristic torsion angles Φ_T and Φ_p in all species to be $+98°$ and $-65°$, respectively, as in the crystal structure of ScPDC (Figure 3). To model the influence of nearby amino acids to the catalytic reaction at a manageable level, we have constructed different model systems with varying residues to reduce the computational cost when different reaction steps were studied. In general, for a specific residue we fixed the position of a non-hydrogen atom (not directly involved in the studied reaction) to be the same as in the crystal structure of the enzyme but let the freedoms of all other atoms to be fully optimized.

To consider the bulk solvent effects of the apoenzyme environment on the energetics of each reaction step, we used the polarizable-continuum model (PCM)[28] to calculate the Gibbs free energy of solvation for each species using its gas-phase-optimized geometry. The free energy of each species in solution is taken as the sum of the gas-phase free energy and the free energy of solvation. The dielectric constant of the apoenzyme environment is typically chosen to be 2−4, which is an average value generated from surrounding protein and water molecules. In our calculations, a dielectric constant of 2.228 was used. For most of species, we have done "frequency" calculations to characterize whether they are minima or transition states and calculate the thermal correction to Gibbs free energies at the temperature of 298 K. Strictly speaking, vibrational frequencies calculated for all optimized geometries with constraints are not true vibrational frequencies. But since there are only a few constraints and these constrained freedoms are not directly involved in the studied reactions, the number of calculated imaginary frequencies could still be used to approximately reflect the nature of the optimized geometry.

It should be mentioned that all species under study exhibit a large number of minima. The structures discussed in the text are not necessarily the absolute minimum of the corresponding species but are believed to be the most likely structures involved in the studied enzyme reaction.

3. Results and Discussions

3.1. Ylide formation. Recent experiments[6,10,12] have demonstrated that the formation of the ylide is an intramolecular proton-transfer process assisted by the imino tautomer of the 4′-aminopyrimidine ring of the ThDP, which is initiated by the hydrogen-bond interaction between the $N_{1'}$ atom and the nearby Glu51 residue. In addition, Gly417 is only 2.83 Å away from the $N_{4'}$ atom of the 4′-amino group in the crystal structure of ScPDC. Hereafter, residues in constructed model systems are designated by their sequences in ScPDC. To probe how the proton transfer from the C_2 atom to the $N_{4'}$ atom is affected by Glu51 or Gly417, we have performed calculations on four different models, with the obtained reactants, transition states, and products displayed in Figure 4. These models differ from each other in the number or type of residues. In these models, the 4′-aminopyrimidine ring of the ThDP is assumed to exist in the imino tautomer, which was experimentally detected.[6,10] Our calculations also demonstrate that with the presence of Glu51 the imino form of the 4′-aminopyrimidine is lower in energy by about 22.2 kcal/mol than its amino tautomeric form. The free energy profiles obtained with these models are shown in Figure 5. Whenever a residue exists in a model, the position of a non-hydrogen atom in this residue, specified by an arrow in Figure 4, is fixed to be the same that as in the X-ray structure of ScPDC. As seen from Figure 4, model **I-a** represents the most realistic model for the enzyme-bound ThDP. Our constrained optimizations lead to a reactant **1-a**, a product **3-a**, and a well-defined transition state **2ts-a**. The calculated distance between the $N_{1'}$ atom and the carboxylic oxygen atom of Glu51 is 2.65 Å for **1-a**, 2.66 Å for **2ts-a**, and 2.69 Å for **3-a**, respectively, being close to the distance of 2.54 Å in the X-ray structure of ScPDC.[7] Clearly, there is a strong hydrogen bond between these two atoms. The interaction between the 4′-amino group and Gly417 is relatively weak, as indicated by the distances between the $N_{4'}$ atom and the carboxylic oxygen atom in these species. The calculated $C_2-N_{4'}$ distance is 2.73, 2.61, and 3.02 Å in **1-a**, **2ts-a**, and **3-a**, respectively. Since the structure of **3-a** should correspond to the crystal structure of ScPDC[7] with the $C_2-N_{4'}$ distance of 3.15 Å, the closeness between the calculated and experimental $C_2-N_{4'}$ distances indicates that model **I-a** is an appropriate model for studying the deprotonation process of the C_2 atom.

However, the calculated $C_{4'}-N_{4'}$ bond length increases from 1.31 Å in **1-a** to 1.35 Å in **3-a**, implying that the aminopyrimidine ring predominantly exists in the imino tautomeric form when the C_2 atom is protonated. The deprotonation of the C_2 atom is calculated to be exothermic by 18.21 kcal/mol, with a free energy barrier of 1.05 kcal/mol. (The barrier of its reverse process is 19.26 kcal/mol.) Thus, the formation of the ylide is thermodynamically favorable and kinetically facile with the presence of both Glu51 and Gly417 residues.

A comparison of results from model **I-b** and model **I−a** shows that the residue Gly417 alone has only a small effect on the proton-transfer barrier in the favorable direction. But Gly417 plays an important role in stabilizing the ylide product, since the exothermicity of the deprotonation step is reduced from 18.21 kcal/mol in model **I-a** to 12.93 kcal/mol in model **I-b**.

However, the absence of the residue Glu51 changes the picture of the ylide formation dramatically, as seen from the results shown in Figure 5. The ylide product becomes less stable than the reactant by 5.51 kcal/mol in the presence of only Gly417 (model **I-c**) or 10.18 kcal/mol in the absence of both Glu51 and Gly417 (model **I-d**). Accordingly, the calculated free energy barrier to yield the ylide is 10.66 kcal/mol for model **I-c** and 12.24 kcal/mol for model **I-d**. Thus, our results demonstrate that the residue Glu51 is essential for accelerating the deprotonation of the C_2 atom and stabilizing the ylide product, and Gly417 plays a secondary role in the ylide formation. These results are consistent with ^{1}H NMR spectroscopy experiments on PDC enzymes and site-specific mutant enzymes.[6,12]

It is interesting how Glu51 contributes so significantly to ylide formation. As seen from the structures obtained from models **I-a** and **I-b**, the transfer of a proton from $N_{1'}$ to one oxygen atom of Glu51 is thermodynamically favorable in all species. From Mulliken charge distributions in the reactants of four different models collected in Table 1, one can see that the $N_{1'}$ atom carries more negative charges (as in **1-a** and **1-b**) when the proton is abstracted by Glu51. The more negatively charged $N_{1'}$ atom induces more charge densities on the $N_{4'}$ atom, which facilitates the proton transfer from the C_2 atom to the $N_{4'}$ atom in the same distance range.

To probe the effect of the protein electrostatic environment on the proton-transfer barrier, we have performed PCM calculations on species **1−3** with different models, with the results shown in Figure 5. In the most realistic model **I-a**, the free energy barrier of the proton transfer in the forward direction is

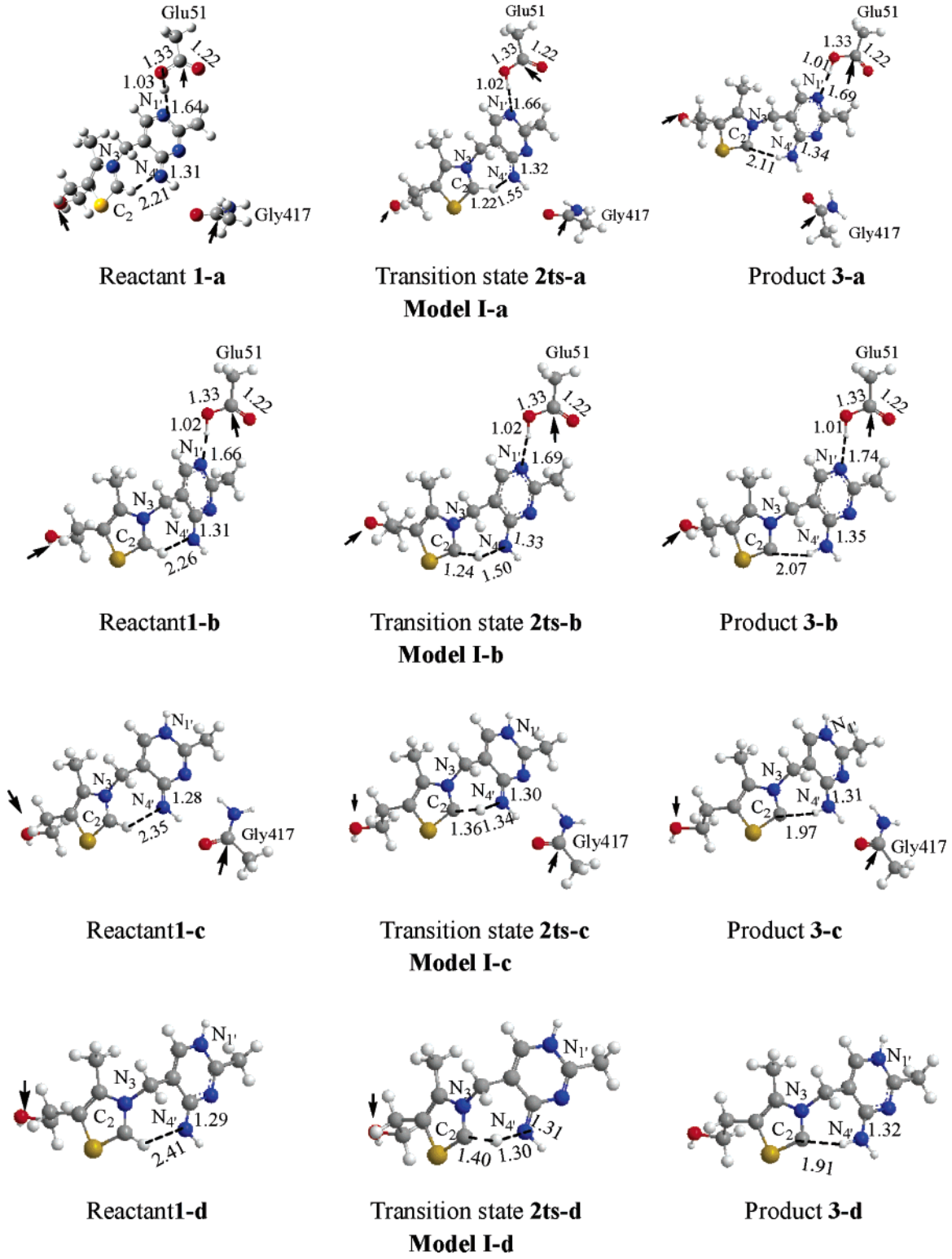

Figure 4. Optimized geometries for ylide formation with different model systems.

calculated to be 2.10 kcal/mol, about 1.0 kcal/mol higher than that in the gas phase. A similar situation occurs in the other three models. Thus, the protein environment has a significant effect on the proton-transfer barrier and thus the rate of ylide formation.

3.2. Covalent Addition of Pyruvate and Decarboxylation of LThDP. Recent ^{1}H NMR spectroscopic analysis of the covalent ThDP intermediates of wild-type ZmPDC and ScPDC enzymes provided direct evidence on the existence of LThDP and HEThDP as intermediates.[14,29] Moreover, the estimated rate constants show that the covalent addition of pyruvate to the C_2 of ThDP to yield enzyme-bound LThDP is very fast, but the decarboxylation process of LThDP is partially rate-limiting in the whole catalytic cycle. Since the energetics of the step to form LThDP depend considerably on how pyruvate approaches ThDP, it is difficult to build a reasonable model system to model this step; thus we will neglect this step. In the following, our study will concentrate on the decarboxylation process of LThDP.

From the active site structure of ScPDC, one can see that Glu477 and Asp28 are within the "striking" distance of the C_2

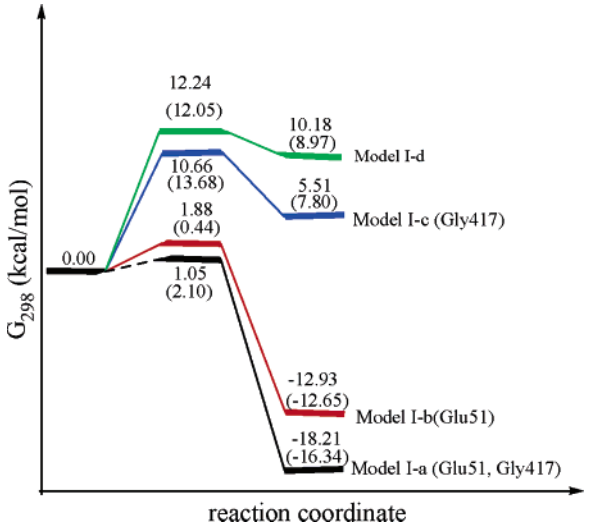

Figure 5. Free energy profiles of ylide formation with different model systems in the gas phase and in the solution phase (values in parentheses).

TABLE 1: Mulliken Atomic Charges in the Reactants with Different Residues

species	$N_{1'}$	$C_{2'}$	$N_{3'}$	$C_{4'}$	$N_{4'}$	C_2	N_3
1-a	−0.590	0.447	−0.541	0.439	−0.724	−0.013	−0.368
1-b	−0.584	0.448	−0.532	0.441	−0.715	−0.010	−0.369
1-c	−0.555	0.511	−0.538	0.455	−0.659	−0.008	−0.376
1-d	−0.547	0.492	−0.499	0.446	−0.646	−0.008	−0.377

atom of the thiazolium ring, and are in a perpendicular orientation to the thiazolium ring. Thus, these two residues are expected to play an important role in the stereochemical control of the decarboxylation of LThDP. The model system (model **II**) constructed for studying the decarboxylation of LThDP is shown in Figure 6. By fixing the positions of those atoms labeled by arrows in Figure 6 and optimizing all other freedoms, we obtained a minimum structure, which corresponds to the reactant **4** (LThDP). In **4**, the calculated bond lengths of C_2-N_3 and $C_2-C_{2\alpha}$ are 1.34 and 1.52 Å, respectively, indicating that the C_2-N_3 bond is a typical double bond and the $C_2-C_{2\alpha}$ bond is a single bond. The distance between a hydrogen atom of Glu477 (or Asp28) and a carboxylate oxygen atom is 1.78 Å (or 1.75 Å), an indication that there is a very strong hydrogen bond between Glu477 (or Asp28) and the carboxylate group. Apparently, the formed hydrogen bonds significantly stabilize the carboxylate anion by inductively withdrawing electrons. The torsion angle $C_{2\beta}-C_{2\alpha}-C_2-S$ is −100°, showing that the $C_{2\beta}-C_{2\alpha}$ σ bond is in a plane almost perpendicular to that of the thiazolium ring. This conformation confirms the "least motion maximum overlap principle" proposed by Kluger et al. for

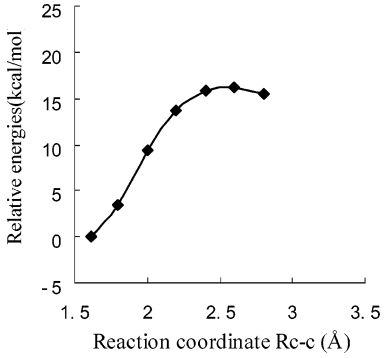

Figure 7. Approximate potential energy profile of the decarboxylation step along the distance between $C_{2\alpha}$ and the carbon atom of CO_2.

enzymatic decarboxylation reactions.[30] However, one should notice that the carbonyl oxygen of pyruvate is spontaneously protonated (which receives a proton from the 4′-amino group) in the course of the covalent binding of pyruvate.

Although many attempts are made to locate the transition state for the decarboxylation step, the transition state is still elusive, probably due to the large structural rearrangement of two surrounding residues during the loss of CO_2. To obtain a rough estimate of the barrier height for the loss of CO_2, we have performed a series of constrained optimizations by fixing the values of the $C_{2\alpha}-CO_2$ distance. The obtained energy change with the variation of the $C_{2\alpha}-CO_2$ distance is plotted in Figure 7. One can see that the decarboxylation step is endothermic, with a barrier of about 16.0 kcal/mol. For the highest point on the potential energy profile, which can be considered as an approximate transition state, its structure (**5**) is shown in Figure 6. In **5**, the $C_{2\alpha}-CO_2$ bond (2.6 Å) is almost broken, and the $C_2-C_{2\alpha}$ bond (1.37 Å) becomes almost a double bond. The protein electrostatic environment would increase this barrier to about 20.0 kcal/mol. This result can be easily understood since the electrostatic environment stabilizes reactant **4** more than the transition state, which is almost neutral. It should be mentioned that when the $C_{2\alpha}-CO_2$ distance reaches 2.80 Å the structure of the CO_2 fragment in LThDP is almost identical to the structure of the isolated CO_2, implying that the loss of CO_2 is almost complete. By removing CO_2 from this structure, we can obtain an approximate structure of the decarboxylation product **6**. (A free optimization would lead to the collapse of this structure, which is not allowed in the enzymatic environment.) The calculated bond lengths clearly show that **6** is a typical enamine compound.

It would be interesting to know the energetics of the decarboxylation reaction in the absence of two nearby residues. Previous theoretical calculations[20] demonstrated that the decarboxylation process would readily proceed through a small barrier

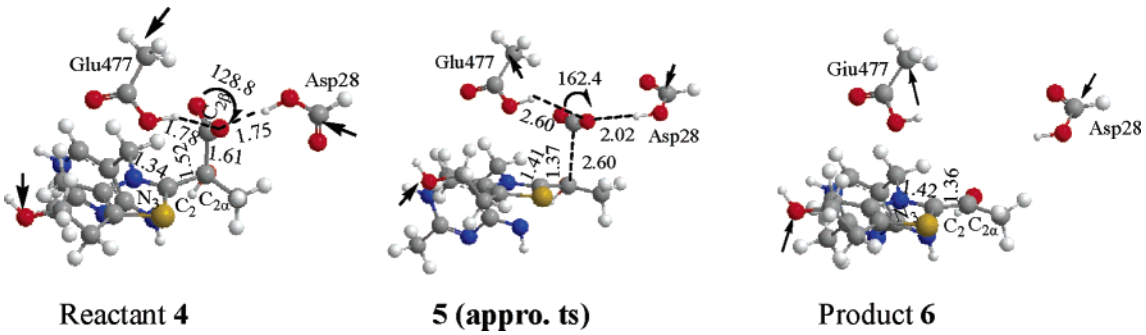

Figure 6. Optimized geometries for the decarboxylation of LThDP. Species **5** corresponds to an approximate transition state, which is obtained from constrained optimizations with the $C_{2\alpha}-CO_2$ distance fixed.

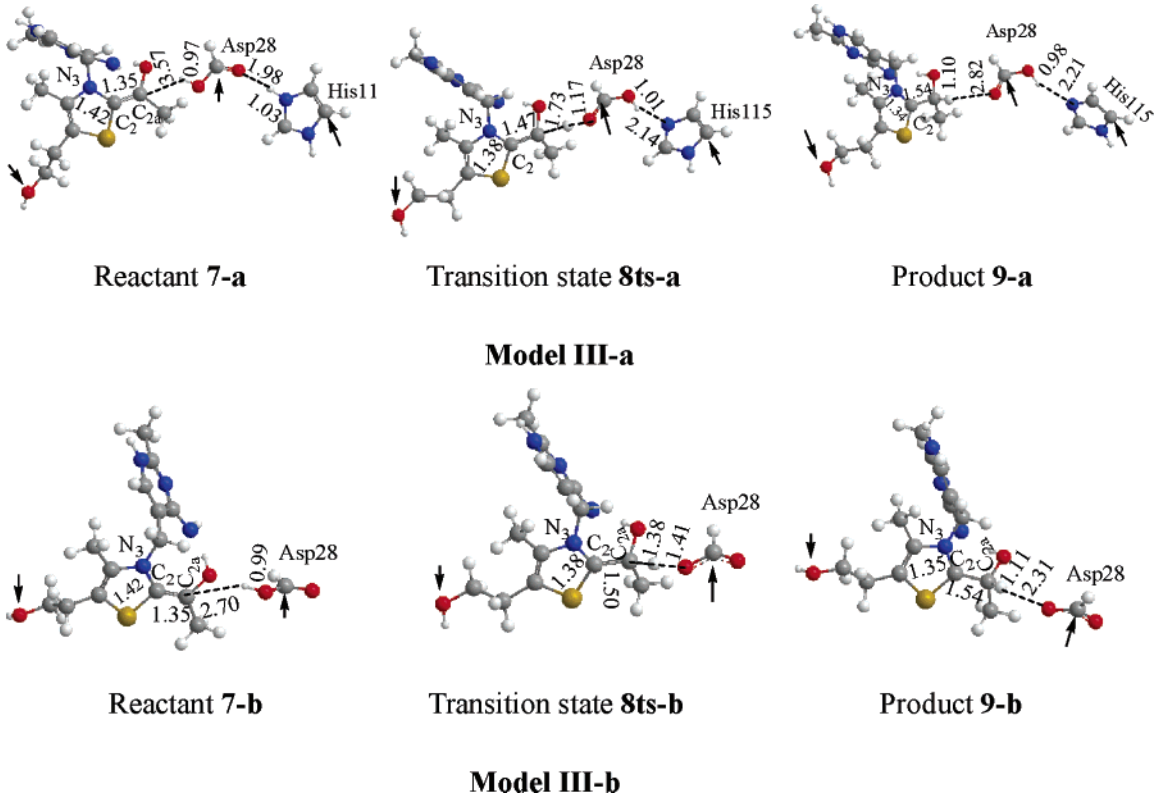

Figure 8. Optimized geometries for the step from enamine to HEThDP.

of less than 5.0 kcal/mol. However, our calculations at the B3LYP/6-31G(d,p) level indicate that without the assistance of two nearby residues LThDP is not a minimum structure.

Instead, the dissociation of CO_2 is spontaneous during the optimization. Thus, in the absence of nearby Glu477 and Asp28 residues, the decarboxylation process should be a barrierless step with strong exothermicity. It should be pointed out that in our calculations LThDP does not exist as a minimum structure, probably because the ThDP moiety is enforced in the V-like conformation.

From model calculations with or without nearby residues, as described above, one can see that both Glu477 and Asp28 residues are very important in the stabilization of the enzyme-bound LThDP and in the stereochemical control of the decarboxylation reaction.

3.3. Formation of HEThDP from the Protonation of the α-Carbanion. As suggested by recent experiments, the His115/Asp28 dyad is likely involved in the formation of HEThDP by providing a proton to the α-carbanion.[14,16,29] As a result, the constructed model system (model **III-a**) including these two residues is shown in Figure 8. (The fixed atom in each residue is labeled by an arrow.) By fixing the freedoms described previously and optimizing all other freedoms, we successfully located two intermediates **7-a** and **9-a**, representing the proton-transfer reactant and product, respectively, and a concerted transition state **8ts-a**, connecting these two species, as shown in Figure 8. From the structure of **8ts-a**, one can see that the transfer of two protons is not precisely synchronous. From the reactant to the transition state, the proton transfer between His115 and Asp28 is almost complete, but the proton transfer between Asp28 and the α-carbanion is still in the early stage. The overall result of this step is that the α-carbanion receives a proton from His115 via the Asp28 bridge. This step is calculated to be exothermic by 18.61 kcal/mol but with a free energy barrier of 33.37 kcal/mol. Single-point PCM calculations

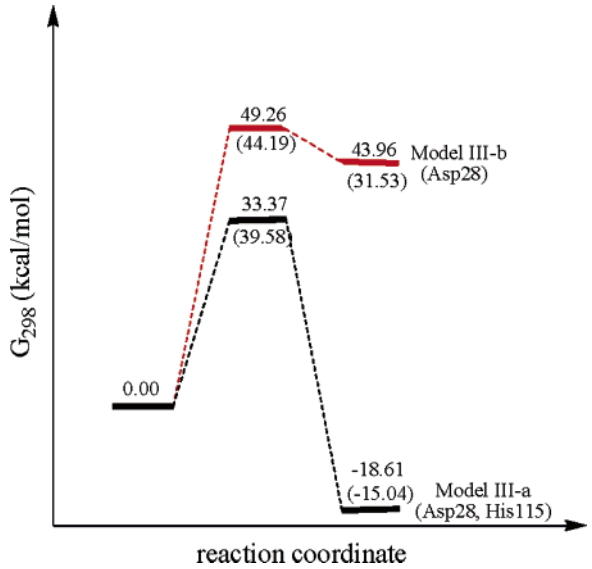

Figure 9. Free energy profiles of the step from enamine to HEThDP with two model systems in the gas phase and in the solution phase (values in parentheses).

show that the protein environment would increase the barrier to 39.58 kcal/mol and reduces the exothermicity to 15.04 kcal/mol.

It is also interesting to investigate whether the protonation of the α-carbanion can occur without the participation of the His115 residue. We have studied this process with the model system **III-b**, with the obtained structures shown in Figure 8. From the corresponding free energy profile in Figure 9, one can notice that the transfer of a proton from Asp28 to the α-carbanion is highly endothermic by 43.96 kcal/mol, with a free energy barrier of 49.26 kcal/mol. The protein environment reduces the endothermicity of this step to 31.53 kcal/mol and

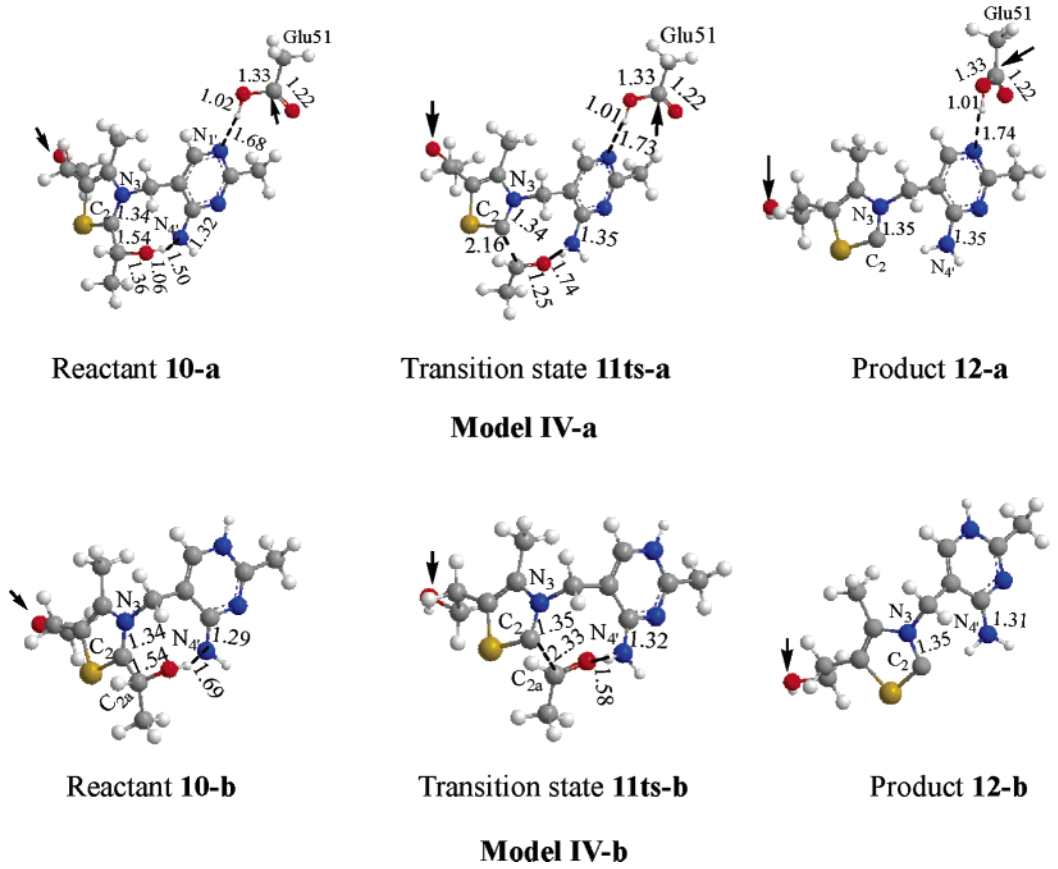

Figure 10. Optimized geometries for acetaldehyde release with two model systems.

the proton-transfer barrier to 44.19 kcal/mol. Clearly, without the presence of His115, the protonation of the α-carbanion is thermodynamically very unfavorable.

A comparison of results from models **III-a** and **III-b** confirms that the protonation of the α-carbanion requires the participation of both residues Asp28 and His115. This result is consistent with the experimental fact that a mutation of either of these two residues slows down the release of acetaldehyde.[14] However, the calculated free energy barrier (about 33 kcal/mol) seems to be somewhat higher than that derived from the experimental rate constant of acetaldehyde release. One would expect that the use of a more realistic model might noticeably reduce the barrier of this step.

3.4. Acetaldehyde Release. The release of acetaldehyde is the last step of the catalytic cycle. Experiments have shown that the α-hydroxyl group of HEThDP must be deprotonated before the elimination of acetaldehyde can occur.[14] The 4′-amino group of the cofactor was suggested to receive a proton from the α-hydroxyl group of HEThDP. From the results in subsection 3.1, one can see that Glu51 plays the most important role in affecting the basicity of the 4′-amino group (Gly417 plays a secondary role). Thus, the minimal realistic model for studying this step is model **IV-a**, as shown in Figure 10.

With model **IV-a**, our optimizations produced a reactant **10-a**, two products **12-a** and acetaldehyde, and a transition state **11ts-a**. The obtained structures of these species are shown in Figure 10, and the corresponding free energy profile is schematically shown in Figure 11. As confirmed by the intrinsic reaction coordinate (IRC) calculations, **11ts-a** is the transition state responsible for acetaldehyde release. From the reactant to the transition state, the $C_2-C_{2\alpha}$ bond length is increased from 1.54 to 2.16 Å, and at the same time, the $C_{2\alpha}-O$ bond is shortened from 1.36 to 1.25 Å, implying that a proton transfer

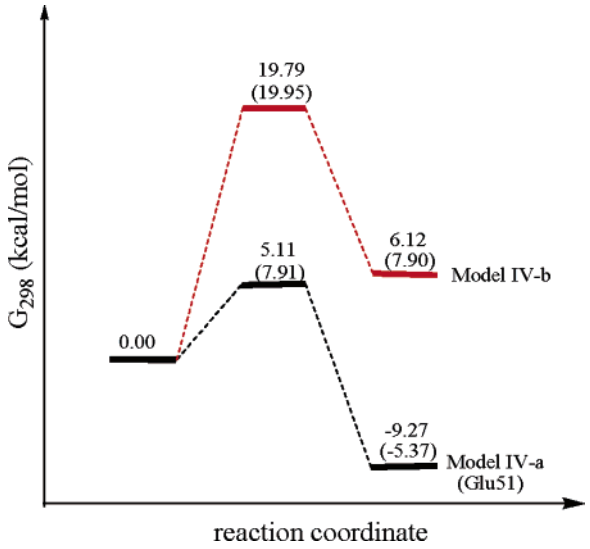

Figure 11. Free energy profiles of acetaldehyde release with different model systems in the gas phase and in the solution phase (values in parentheses).

from the α-hydroxyl group to the 4′-amino group is almost complete. Thus, **11ts-a** involves the concerted motion of the $C_2-C_{2\alpha}$ breaking and the deprotonation of the α-hydroxyl group, although these two movements are not precisely synchronous. The regeneration of the ylide product **12-a** completes the whole catalytic cycle. The acetaldehyde release step is calculated to be exothermic by 9.27 kcal/mol with a free energy barrier of 5.11 kcal/mol. Single-point PCM calculations show that the protein environment would increase the barrier of this step to 7.91 kcal/mol but decrease the exothermicity to 5.37 kcal/mol.

Let us investigate how the energetics of acetaldehyde release are affected by the absence of Glu51. We have performed calculations on the model system **IV-b**, with the obtained structures shown in Figure 10. The structures of these species are quite similar to the corresponding structures obtained with model **IV-a**, except that the geometrical parameters of the aminopyrimidine ring show noticeable distinction between the corresponding species. From Figure 11, it can be seen that without the assistance of Glu51 the loss of acetaldehyde is endothermic by 6.12 kcal/mol and has to overcome a free energy barrier as high as 19.79 kcal/mol. After the solvation energies caused by the protein electrostatic environment are considered, the endothermicity of this step becomes 7.90 kcal/mol, but the barrier of this step remains almost unchanged.

By comparing results from models **IV-a** and **IV-b**, one can see that the residue Glu51 plays a very important role in accelerating the release of acetaldehyde through the proton relay between Glu51, $N_{1'}$, and the 4′-amino group of ThDP. This result accounts well for the experimental fact that a mutation of Glu50 drastically decreases the rate of acetaldehyde release in ZmPDC. (Glu50 corresponds to Glu51 in ScPDC.[14])

4. Conclusions

In this work, we have presented a comprehensive theoretical investigation on the mechanisms of all elementary reaction steps involved in the catalytic cycle of PDC. Different minimal realistic models are constructed for mimicking the involvement of some key residues in a certain step. Especially, the contribution of an individual residue to a certain step is estimated from calculations on model systems with and without this residue. To mimic the effect of the protein framework on the structures of model systems and thus on the energetics of individual catalytic steps, the cofactor ThDP is set to be in its V-like conformation as in the crystal structure of ScPDC, and each residue in the active site is partially constrained by fixing the position of a non-hydrogen atom to be the same as that in the crystal structure of ScPDC. In addition, the effect of the rest apoenzyme environment on each catalytic step is treated by the self-consistent reaction field method.

Several conclusions can be drawn from our calculations with respect to the mechanisms of individual steps in the catalytic cycle. First, the proton relay between Glu51, $N_{1'}$, and the 4′-amino group of ThDP is computationally confirmed. Thus, the presence of Glu51 is essential for the deprotonation step of the C_2 atom and the release of acetaldehyde, in both of which the $N_{4'}$ atom of the 4′-amino group receives a proton. With the presence of both Glu51 and Gly417 residues, the formation of the ylide is calculated to be exothermic by 18.21 kcal/mol with a free energy barrier of 1.05 kcal/mol. Second, the presence of Glu477 and Asp28 residues makes the decarboxylation of LThDP an endothermic process, with an approximate barrier of about 16 kcal/mol. In the absence of these two residues, the decarboxylation step should be barrierless and strongly exothermic. Third, the protonation of the α-carbanion is found to go through a concerted transition state involving both Asp28 and His115 residues. This step is exothermic by 18.61 kcal/mol but with a free energy barrier of 33.37 kcal/mol. Without the existence of His115, the protonation of the α-carbanion is thermodynamically inaccessible. Fourth, the release of acetaldehyde is likely to proceed through a concerted transition state involving $C_2-C_{2\alpha}$ bond-breaking and the deprotonation of the α-hydroxyl group. With the assistance of Glu51, this step is an exothermic process with a free energy barrier of 5.11 kcal/mol. Otherwise, this step becomes endothermic by 6.12 kcal/mol. Although the solvent effect caused by the protein electrostatic environment does shift the energy barrier and the endothermicity or exothermicity of each step by a few kcal/mol, the basic feature of the potential energy profiles of each step captured from gas-phase calculations remains the same. From comparisons of the energetics of individual steps, one can see that the decarboxylation of LThDP and the protonation of the α-carbanion are two rate-limiting steps, while the ylide formation and the release of acetaldehyde should be relatively fast. This result can give a satisfactory explanation for the relatively small rate constants experimentally measured for both decarboxylation and acetaldehyde release. (The protonation of the α-carbanion is considered by experimentalists as a part of the acetaldehyde release step.[14]) Moreover, the catalytic roles of residues Glu51, Glu477, Asp28, and Gly417 in the active site of ScPDC in single steps elucidated from our present study are also in good agreement with those derived from site-directed mutagenesis on the enzyme ZmPDC.[15−17]

Although we have made significant progress in understanding the catalytic mechanism of PDC at a molecular level, it is important to point out some limitations inherent in this study. First, for some steps the model systems that we built are not large enough for quantitative estimates of their energetics. For instance, the calculated barrier (about 33 kcal/mol) for the protonation of the α-carbanion is somewhat higher than that expected from experiments. This might be partially due to the fact that another residue His114, which is 4.13 Å away from His115 in the crystal structure of ScPDC, is not explicitly considered in the corresponding model system. Second, in our calculations the effect of the protein framework on the potential energy profiles of active site models is approximately modeled by fixing some freedoms. Although this approximation is reasonable for cases in which one or two residues are primarily involved in a certain step, it may give rise to relatively large deviations from the realistic situation for other cases. At the present time, another way for studying the enzymatic reactions is the combination of the quantum mechanics/molecular mechanics (QM/MM) method with sufficiently large active site models, which will be used in our future work.

Acknowledgment. This work was supported by the National Basic Research Program (Grant Nos. 2004CB719901 and 2003CB114400) and the National Natural Science Foundation of China (Grant Nos. 20373022 and 20233020).

Supporting Information Available: Total electronic energies, gas-phase free energies, the solvation free energies, and the Cartesian coordinates of all stationary points under study. This material is available free of charge via the Internet at http://pubs.acs.org.

References and Notes

(1) Krampitz, L. O. *Annu. Rev. Biochem.* **1969**, *38*, 213.

(2) Jordan, F.; Nemeria, N.; Guo, F.; Baburina, I.; Gao, Y.; Kahyaoglu, A.; Li, H.; Wang, J.; Yi, J.; Guest, J.; Furey, W. *Biochim. Biophys. Acta* **1998**, *1385*, 287.

(3) Dobritzsch, D.; Konig, S.; Schneider, G.; Lu, G. *J. Biol. Chem.* **1998**, *273*, 20196.

(4) Breslow, R. *J. Am. Chem. Soc.* **1958**, *80*, 3719.

(5) Alvarez, F. J.; Ermer, J.; Hübner, G.; Schellenberger, A.; Schowen, R. L. *J. Am. Chem. Soc.* **1991**, *113*, 8402.

(6) Kern, D.; Kern, G.; Neef, H.; Tittmann, K.; Killenberg-Jabs, M.; Schneider, C. W.; Hübner, G. *Science* **1997**, *275*, 67.

(7) Arjunan, P.; Umland, T.; Dyda, F.; Swaminathan, S.; Furey, W.; Sax, M.; Farrenkopf, B.; Gao, Y.; Zhang, D.; Jordan, F. *J. Mol. Biol.* **1996**, *256*, 590.

(8) Schelleenberger, A. *Angew. Chem.* **1967**, *79*, 1050.

(9) Muller, Y. A.; Lindqvist, Y.; Furey, W.; Schulz, G. E.; Jordan, F.; Schneider, G. *Structure* **1993**, *1*, 95.

(10) Jordan, F.; Nemeria, N. S.; Zhang, S.; Yan, Y.; Arjunan, P.; Furey, W. *J. Am. Chem. Soc.* **2003**, *125*, 12732.

(11) Lobell, M.; Crout, D. H. G. *J. Am. Chem. Soc.* **1996**, *118*, 1867.

(12) Killenberg-Jabs, M.; Konig, S.; Eberhardt, I.; Hohmann, S.; Huber, G. *Biochemistry* **1997**, *36*, 1900.

(13) Ragsdale, S. W. *Chem. Rev.* **2003**, *103*, 2333.

(14) Tittmann, K.; Golbik, R.; Uhlemann, K.; Khailova, L.; Schneider, G.; Patel, M.; Jordan, F.; Chipman, D. M.; Duggleby, R. G.; Hübner, G. *Biochemistry* **2003**, *42*, 7885.

(15) Liu, M.; Sergienko, E. A.; Guo, F.; Wang, J.; Tittmann, K.; Hübner, G.; Furrey, W.; Jordan, F. *Biochemistry* **2001**, *40*, 7355.

(16) Sergienko, E. A.; Jordan, F. *Biochemistry* **2001**, *40*, 7369.

(17) Sergienko, E. A.; Jordan, F. *Biochemistry* **2001**, *40*, 7382.

(18) Kluger, R. *Chem. Rev.* **1987**, *87*, 863.

(19) Jordan, F.; Nemeria, N. S.; Zhang, S.; Yan, Y.; Arjunan, P.; Furey, W. *J. Am. Chem. Soc.* **1974**, *96*, 3623.

(20) Friedemann, R.; Breitkopf, C. *Int. J. Quantum Chem.* **1996**, *57*, 943.

(21) Sakaki, S.; Musashi, Y.; Ohkubo, K. *J. Am. Chem. Soc.* **1993**, *115*, 1515.

(22) Friedemann, R.; Neef, H. *Biochim. Biophys. Acta* **1998**, *1385*, 245.

(23) Friedemann, R.; Tittmann, K.; Golbik., R.; Hübner, G. *Int. J. Quantum Chem.* **2004**, *99*, 109.

(24) Friedemann, R.; Fircks, A. V.; Naumann, S. *Int. J. Quantum Chem.* **1998**, *70*, 407.

(25) Friedemann, R.; Naumann, S. *J. Mol. Struct.: THEOCHEM* **2003**, *630*, 275.

(26) Shin, W.; Oh, D.-G.; Chae, C.-h.; Yoon, T.-s. *J. Am. Chem. Soc.* **1993**, *115*, 12238.

(27) Frisch, M. J.; Trucks, G. W.; Schlegel, H. B.; Scuseria, G. E.; Robb, M. A.; Cheeseman, J. R.; Montgomery, J. A., Jr.; Vreven, T.; Kudin, K. N.; Burant, J. C.; Millam, J. M.; Iyengar, S. S.; Tomasi, J.; Barone, V.; Mennucci, B.; Cossi, M.; Scalmani, G.; Rega, N.; Petersson, G. A.; Nakatsuji, H.; Hada, M.; Ehara, M.; Toyota, K.; Fukuda, R.; Hasegawa, J.; Ishida, M.; Nakajima, T.; Honda, Y.; Kitao, O.; Nakai, H.; Klene, M.; Li, X.; Knox, J. E.; Hratchian, H. P.; Cross, J. B.; Bakken, V.; Adamo, C.; Jaramillo, J.; Gomperts, R.; Stratmann, R. E.; Yazyev, O.; Austin, A. J.; Cammi, R.; Pomelli, C.; Ochterski, J. W.; Ayala, P. Y.; Morokuma, K.; Voth, G. A.; Salvador, P.; Dannenberg, J. J.; Zakrzewski, V. G.; Dapprich, S.; Daniels, A. D.; Strain, M. C.; Farkas, O.; Malick, D. K.; Rabuck, A. D.; Raghavachari, K.; Foresman, J. B.; Ortiz, J. V.; Cui, Q.; Baboul, A. G.; Clifford, S.; Cioslowski, J.; Stefanov, B. B.; Liu, G.; Liashenko, A.; Piskorz, P.; Komaromi, I.; Martin, R. L.; Fox, D. J.; Keith, T.; Al-Laham, M. A.; Peng, C. Y.; Nanayakkara, A.; Challacombe, M.; Gill, P. M. W.; Johnson, B.; Chen, W.; Wong, M. W.; Gonzalez, C.; Pople, J. A. *Gaussian 03*, revision B.04; Gaussian, Inc.: Wallingford, CT, 2004.

(28) Tomasi, J.; Persico, M. *Chem. Rev.* **1994**, *94*, 2027.

(29) Schütz, A.; Golbik, R.; Konig, S.; Hübner, G.; Tittmann, K. *Biochemistry* **2005**, *44*, 6164.

(30) Turano, A.; Furey, W.; Pletcher, J.; Sax, M.; Pike, D.; Kluger, R. *J. Am. Chem. Soc.* **1982**, *104*, 3089.